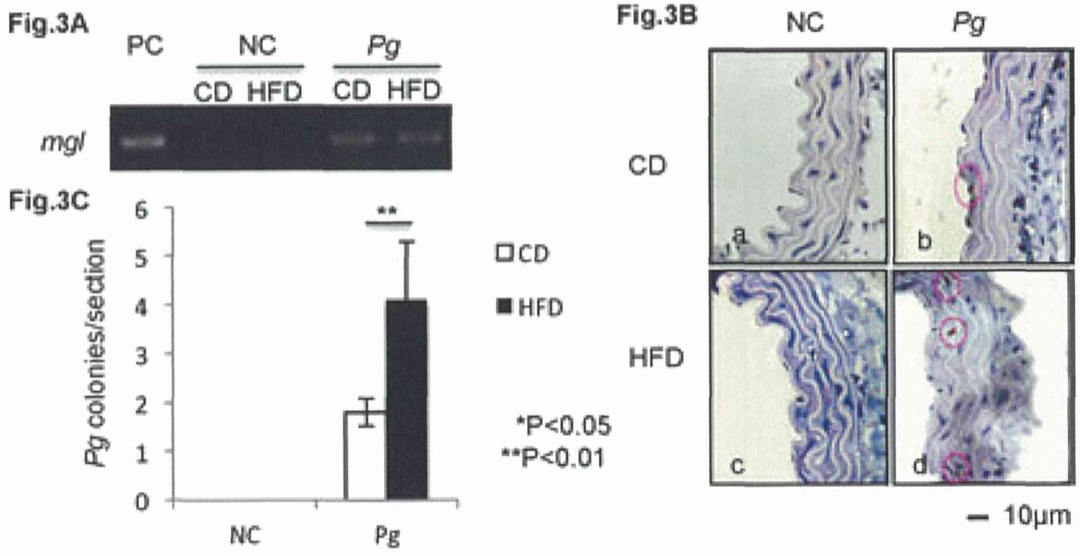

Figure 3. Dental *Pg* infection predisposes to increased invasion of injured mouse aortal tissue under HFD conditions. (A) Expression of the mgl gene of *Pg* is detected in aortal tissue of infected mice. Genomic DNA of *Pg* W83 strain is included as a positive control (PC). (B) Immunolocalization of *Pg* (brown particles) is observed in aortal walls of infected mice. (C) *Pg* invasion is significantly higher in HFD-*Pg* group. Mean ± SD *P<0.05, **P<0.01. Scale bar, 10 μm; CD, chow diet; HFD, high fat diet; NC, negative control; *Pg, Porphyromonas gingivalis.* Experiments were performed three times or more with similar results.
doi:10.1371/journal.pone.0110519.g003

palmitate (Figure 5A). Effects of *Pg*-LPS on expression of inflammation associated factors COX-2 (a synthetic enzyme of inducible PGE_2) and TNF-α. *Pg*-LPS induced a slight increase in COX-2 mRNA, and a more robust increase in TNF-α in HuhT1 cells Palmitate treatment alone increased TNF-α expression. Unexpectedly, 1 h of *Pg* whole cell priming on HuhT1 cells did not alter the mRNA expression of COX-2 and TNF-α. In the palmitate pre-treated group, expression of both COX-2 and TNF-α were strongly enhanced by *Pg*-LPS stimulation and only TNF-α mRNA was increased by Pg whole cell stimulation (Figure 5B).

Palmitate increases *Pg* cell invasion in HuhT1 cells (Figure 6)

The antibiotic protection assay was performed to determine whether *Pg* cells were capable of invading and remaining viable within HuhT1 cells, *in vitro*. Immunofluorescent staining exhibited the existence of invaded *Pg* shown in green in HuhT1 cells (Figure 6A). Brown *Pg* colonies appeared 5 days post plating on blood agar (data not shown). Pretreatment of cells with 50 μM palmitate significantly increased the number of invading *Pg* colonies in HuhT1 cells (P<0.01) (Figure 6B).

Discussion

The health of the inner arterial wall is an important factor in preventing vascular disease development. However, the endothelium is easily damaged by various atherogenic factors, including hypercholesterolemia, homocysteine, oxidative stress, and hyperglycemia [19]. To study the effect of dental infection on endothelial injury associated with obesity, we induced obesity in mice by high fat diet feeding, and then applied *Pg* bacteria to pulp chambers of upper molars.

The relationship between periodontitis and systemic disease has been the subject of intense speculation and research in recent years. Periodontitis, a bacterially induced inflammatory disease, destroys the periodontal tissues and may ultimately lead to tooth exfoliation. Among the over 700 bacterial species colonizing the oral cavity [20], *Pg* is highly detectable in the periodontal pocket during chronic periodontitis, and is considered to be one of the principal bacterial species responsible for inducing periapical periodontitis [11–13]. *Pg* is a Gram-negative species that requires anaerobic conditions for growth. In our mouse model, we delivered *Pg* into pulp chambers, providing a natural route for infection to induce periapical periodontitis. Dental infection by *Pg* caused total pulp necrosis and establishment of periapical granuloma, in which *Pg* was detected in neutrophils and macrophages. Previously, we have shown using this mouse model that *Pg* colonies remained viable inside infected pulp chambers and that bacteria were able to reproduce over a long period of time to induce periapical periodontitis, affecting the pathological progression of nonalcoholic steatohepatitis [21]. In this model, we hypothesize that the periapical granulomas are a stable and persistent source of the *Pg* and its immunogenic products, allowing spreading through the bloodstream.

In the mouse model used in the present study, the reduced expression of endothelial marker CD31 and increased presence of TUNEL staining revealed the loss of endothelial integrity, identifying endothelial injury in the HFD-NC group compared with the CD-NC group (Figure 2). In addition, the body weight, epididymal fat weight, and total cholesterol were elevated in HFD-fed mice (Table S1), confirming the establishment of dyslipidemia caused by obesity. Correspondingly, using the diet-induced atherosclerotic rabbit model, Yu *et al.* reported that long term (16 weeks) feeding of HFD induced loss of integrity in the endothelial layer [22]. According to Boden *et al.* FFAs appear to be a major link between obesity and the development of atherosclerotic vascular disease [23]. *In vitro* studies showed that FFA treatment would induce apoptosis of various cells, including endothelial cells [24], and accelerated apoptosis likely contributes to the loss of endothelial integrity, in turn leading to increased permeability. In these studies, we additionally demonstrate palmitate-induced higher affinity to Annexin V and PARP cleavage in HuhT1 cells (Figure 4C, 4D, 4E), indicating that

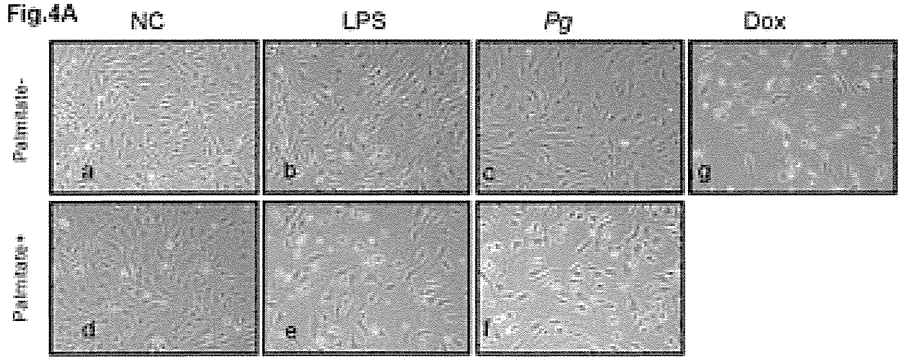

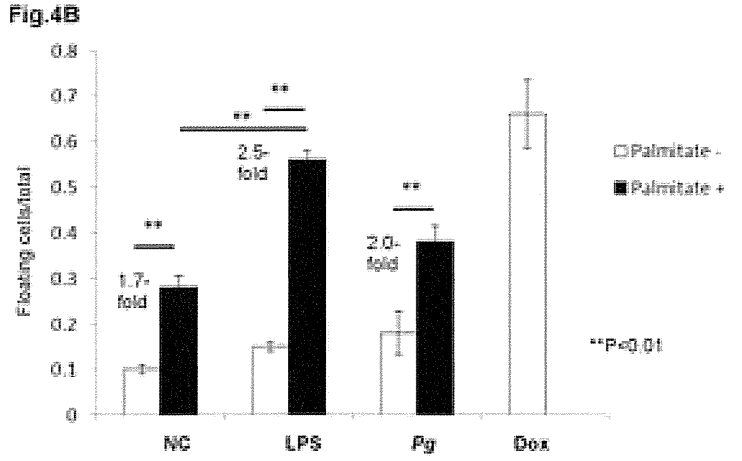

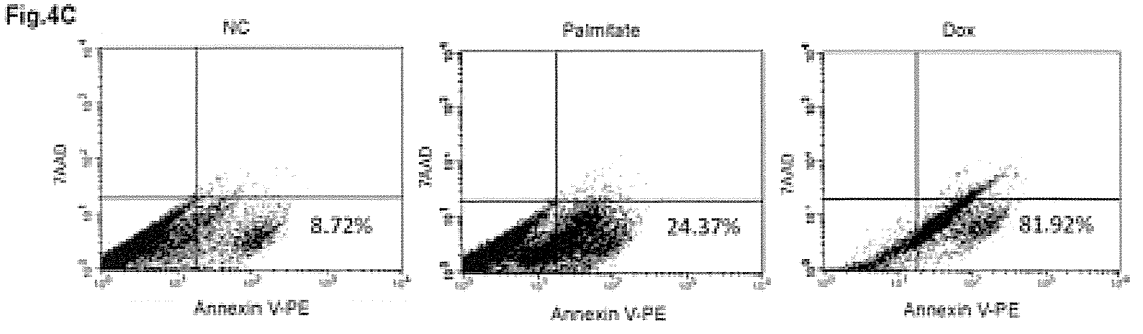

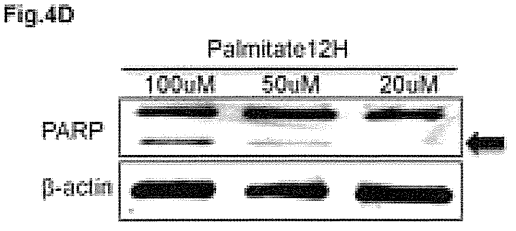

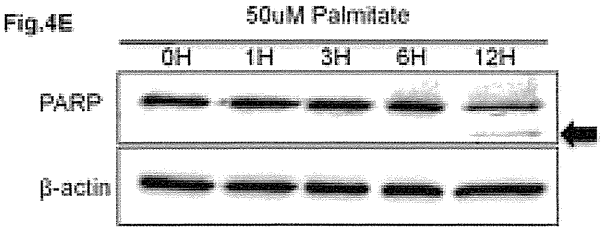

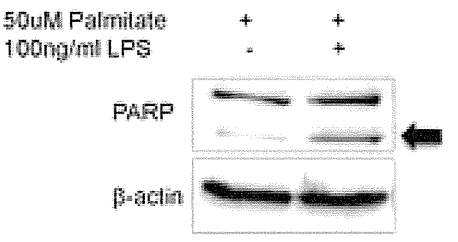

Figure 4. *Pg* and *Pg*-LPS increase palmitate-induced apoptosis in HuhT1 cells. (A, B) Palmitate treatment induces HuhT1 cell detachment, and *Pg* and/or *Pg*-LPS treatment further increases detachment. (C) Palmitate stimulation induces cell death by apoptosis that is indicated by increased percentage of Annexin V positive cells; Dox is positive control. (D, E) Palmitate stimulation induces PARP cleavage (arrow, cleaved PARP) in HuhT1

cells in a dose- and time-dependent manner. (F) *Pg*-LPS accelerates PARP cleavage in palmitate-treated cells. Mean ± SD, **P<0.01. NC, negative control; *Pg, Porphyromonas gingivalis*; PARP, Poly (ADP-ribose) polymerase; Dox, Doxorubicin. Experiments were performed three times or more with similar results.
doi:10.1371/journal.pone.0110519.g004

increased apoptosis is a potential mechanism for FFA-induced endothelial cell layer injury.

In the HFD groups, addition of *Pg* further reduced expression of CD31 and increased presence of TUNEL positive cells in the endothelial layer, compared to the non-*Pg*-treated controls. CD31 is an adhesion molecule expressed on endothelial cells that is important for maintaining endothelial integrity [25] and facilitates transendothelial migration of neutrophils to sites of inflammation [26]. Carrithers *et al.* revealed that CD31-deficient mice showed enhanced vascular permeability and increased apoptotic endothelial cell death during LPS-induced shock, compared to wild type controls, suggesting that CD31 is necessary for maintenance of endothelial integrity and prevention of apoptosis [27]. *Pg* infection increases serum levels of LPS in our animal model [21]. In the *in vitro* portion of these studies, we observed that addition of *Pg*-LPS to HuhT1 cells significantly increased cell detachment with FFA pre-stimulation (Figure 4B). Furthermore, PARP cleavage clearly showed that *Pg*-LPS promoted cell apoptosis with FFA pre-treatment (Figure 4F). For future studies, it will be of interest to investigate the role of CD-31 in LPS- and FFA-induced endothelial cell apoptosis. Interestingly, although the HFD-*Pg* *in vivo* exhibited most severe endothelial injury and highest number of *Pg* colonies in aorta, the effect of *Pg* whole cell was not as robust as *Pg*-LPS in inducing endothelial cell death with addition of FFA. Yun *et al.* reported that gingipains (major virulence determinants) of *Pg* may contribute to the initiation of endothelial barrier destruction by cleaving CD31 at the endothelial cell-cell junction, eventually resulting in increased vascular permeability [28]. The *Pg* invasion in aortal wall observed in the current study may be the consequence of increased vascular permeability induced by degradation of CD31, probably through gingipains. However, a better understanding of this mechanism requires further investigation.

TNF-α is one of the key cytokines in inflammatory pathologies, stimulating the production of other proinflammatory cytokines, chemokines, and also COX-2, consequently contributing to endothelial cells apoptosis [29]. In the present study, a single *Pg*-LPS or FFA treatment increased COX-2 and TNF-α gene expression in endothelial cells. It is reported that palmitate activates NF-κB and increases inflammatory cytokine production via TLR4 in endothelial cells and adipocytes, which is consistent with our result [30,31]. Interestingly, *Pg*-LPS stimulation dramatically up-regulated COX-2 and TNF-α gene expression in FFA-pretreated endothelial cells (Figure 5). To our knowledge, this is the first demonstration of a combined effect of *Pg*-LPS and FFA on inflammatory mediator production and endothelial cell apoptosis, though more work will be done to show whether the effect is additive or synergystic. As both FFA and LPS are ligands to TLR4 and could induce proinflammatory cytokines through the NF-κB pathway [32,33], the cooperative effect of FFA and *Pg*-LPS on TNF-α up-regulation may be due to the co-activation of NF-κB pathway via TLR4. It is known that *in vivo*, proinflammatory cytokines produced in response to FFA contribute to low-grade inflammation in fat, liver, and the aortal wall [34,35], and we

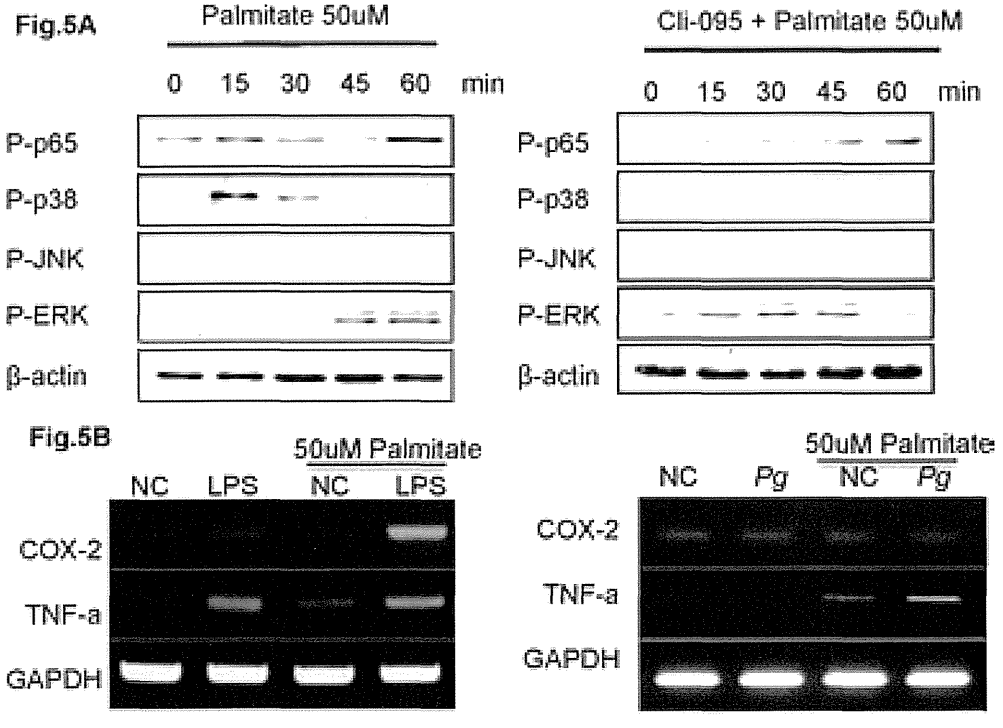

Figure 5. *Pg*-LPS up-regulates COX-2 and TNF-α expression in palmitate treated HuhT1 cells. (A) Phosphorylation of p65, p38, JNK and ERK was detected by western blotting. Cells were pretreated with Cli-095 6 h before palmitate stimulation. (B) mRNA expression of COX-2 and TNF-α in HuhT1 cells with and without palmitate treatment at 1 h after Pg and/or *Pg*-LPS stimulation. NC, negative control; *Pg, Porphyromonas gingivalis*; Cli-095, TLR4 inhibitor. Experiments were performed three times or more with similar results.
doi:10.1371/journal.pone.0110519.g005

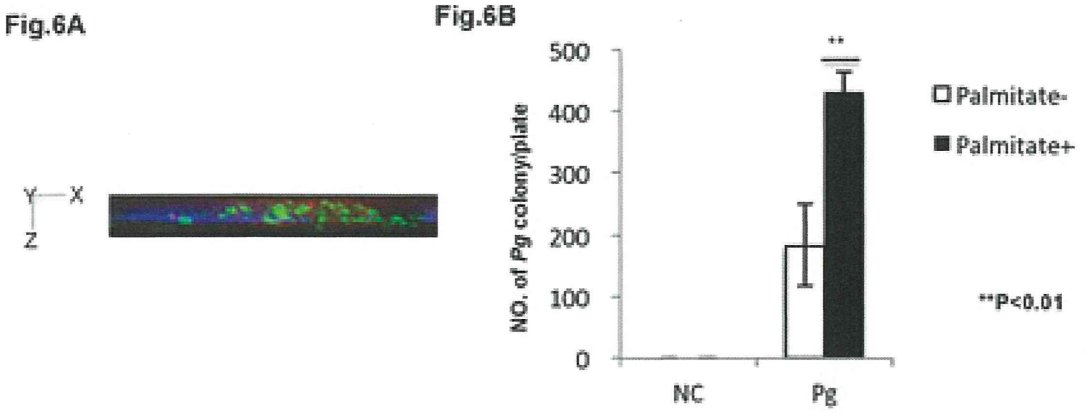

Figure 6. Palmitate increases *Pg* cell invasion in HuhT1 cells. Antibody protection assay (see Material & Methods) was used to determine *Pg* invasion in HuhT1 cells. (A) Invaded *Pg* was analyzed by fluorescent microscopy at magnification of 1000x. Side view (X–Z plane) is shown. *Pg* (green); DAPI (blue); Phalloidin (red). (B) *Pg* invasion into HuhT1 cells is increased under palmitate pre-treatment. Mean ± SD, **P<0.01. NC, negative control; *Pg Porphyromonas gingivalis*. Experiments were performed three times or more with similar results.
doi:10.1371/journal.pone.0110519.g006

propose that *Pg*-LPS exacerbates the inflammation in the aortal wall by further up-regulating cytokines. This is supported by the immunohistochemical staining and RT-PCR detection of *Pg* colonies in aortal wall of infected mice (Figure 3). Furthermore, we demonstrated that there is a significant difference between CD-*Pg* and HFD-*Pg* referring the tissue invasion rate by applying equal amount of *Pg* from pulp chamber (Figure 3C). Correspondingly, our *in vitro* study showed that *Pg* easily invaded damaged HuhT1 endothelial cells following FFA pretreatment. Several reports demonstrated the detection of DNA of *Pg* and *Aggregatibacter actinomycetemcomitans* (*Aa*) in atheromatous plaque, with *Pg* (78.57%) as the most commonly found periodontal pathogens followed by *Aa* (66.67%) [36]. These findings point to the capability for periodontal pathogens to access systemic circulation, colonize distant sites such as the aortal wall, and influence the pathophysiology of atherogenesis.

Based on these previous findings and data generated in the current study, we hypothesize that *Pg*-LPS may exacerbates FFA-induced endothelial injury in aortal walls of obese individuals, providing easy access for circulating *Pg* to invade and colonize the deep intima and promote the development of atherosclerosis through additive local production of pro-inflammatory cytokines. However, further investigations will help clarify the effect of *Pg* infection on endothelial cells and smooth muscle cells in the aortal wall.

In summary, data from this study demonstrate that *Pg* from a dental infection are capable of invading aortal tissue through the circulation and exacerbating HFD-induced endothelial damage, in part by accelerating endothelial cell apoptosis. On the other hand, HFD-induced endothelial damage enhanced *Pg* invasion rate. Furthermore, FFAs contributed to the up-regulation of inflammation and apoptosis of endothelial cells, and *Pg*-LPS aggravated this effect. Taken together, this is the first demonstration that dental infection of *Pg* can contribute to endothelial injury in obese mice. Extrapolation these results suggests that careful attention to dental hygiene or periodontal treatment and maintenance may be beneficial for obese patients in order to prevent or minimize adverse effects of bacterial infection on the early stages of atherosclerosis.

Supporting Information

Table S1 Establishment of dyslipidemia in HFD-fed mice. Body weight, epididymal fat weight and total cholesterol were measured in four groups of mice (CD-NC, CD-*Pg*, HFD-NC and HFD-*Pg*); $^{a}p<0.01$ to CD-NC, $^{b}p<0.01$ to CD-*Pg*, $^{c}p<0.05$ to CD-NC and $^{d}p<0.05$ to CD-*Pg*. CD, chow diet; HFD, high fat diet; NC, negative control; *Pg, Porphyromonas gingivalis*. Experiments were performed three times with similar results.
(TIF)

Acknowledgments

We thank Dr. Junzou Hisatune (Department of Bacteriology, Hiroshima University, Japan) for providing *Pg* cultures, Dr. Kazuhisa Ouhara (Department of Periodontal Medicine, Hiroshima University, Japan) for providing PCR primer pairs for mgl. We would also like to thank Dr. Brian Foster (Laboratory of Oral Connective Tissue Biology, NIAMS, National Institutes of Health) for language editing.

Author Contributions

Conceived and designed the experiments: MA MM TT. Performed the experiments: MA MM TI MK HF TA NFA AN. Analyzed the data: MA MM KK. Contributed reagents/materials/analysis tools: KI HT. Contributed to the writing of the manuscript: MA MM TT.

References

1. Ross R, Harker L (1976) Hyperlipidemia and atherosclerosis. Science 193(4258): 1094–100.
2. Fuster V, Kelly BB, editors (2010) Promoting Cardiovascular Health in the Developing World: A Critical Challenge to Achieve Global Health. Washington (DC): National Academies Press (US).
3. Libby P (2012) Inflammation in atherosclerosis. Arterioscler Thromb Vasc Biol 32(9): 2045–51. doi:10.1161/ATVBAHA.108.179705.
4. Ross R (1999) Atherosclerosis is an inflammatory disease. Am Heart J 138(5 Pt 2): S419–20.
5. Tritto I, Ambrosio G (2004) The multi-faceted behavior of nitric oxide in vascular "inflammation": catchy terminology or true phenomenon? Cardiovasc Res 63(1): 1–4.
6. Shah PK (1999) Plaque disruption and thrombosis Potential role of inflammation and infection. Cardiol Clin 17(2): 271–81.
7. Libby P, Egan D, Skarlatos S (1997) Roles of infectious agents in atherosclerosis and restenosis: an assessment of the evidence and need for future research. Circulation 96(11): 4095–103.
8. Kuvin JT, Kimmelstiel CD (1999) Infectious causes of atherosclerosis. Am Heart J 137(2): 216–26.

9. Wang Z, Zhang M, Yu Z, Shui Y, Ding Y, et al. (2012) An animal experiment study on the effect of periodontitis on atherosclerosis. Hua Xi Kou Qiang Yi Xue Za Zhi 30(3): 308–13.
10. Cai Y, Kurita-Ochiai T, Hashizume T, Yamamoto M (2012) Green tea epigallocatechin-3-gallate attenuates Porphyromonas gingivalis-induced atherosclerosis. *FEMS Immunol Med Microbiol* Sep 11. doi:10.1111/1574-695x.12001.
11. Yang HW, Huang YF, Chou MY (2004) Occurrence of Porphyromonas gingivalis and Tannerella forsythensis in periodontally diseased and healthy subjects. J Periodontol 75: 1077–1083.
12. Saito D, Coutinho LL, Borges Saito CP, Tsai SM, Hofling JF (2009) Real-time polymerase chain reaction quantification of Porphyromonas gingivalis and Tannerella forsythia in primary endodontic infections. J Endod 35(11): 1518–24. doi:10.1016/j.joen.2009.08.005.
13. Pereira CV, Stipp RN, Fonseca DC, Pereira LJ, Hofling JF (2001) Detection and clonal analysis of anaerobic bacteria associated to endodontic-periodontal lesions. J Periodontol 82: 1767–1775. doi:10.1902/jop.2011.110063. Epub 2011 Mar 29.
14. Yoshimura M, Nakano Y, Yamashita Y, Oho T, Saito T (2000) Formation of methyl mercaptan from L-methionine by Porphyromonas gingivalis. Infect Immun 68: 6912–6916.
15. Anno K, Hayashi A, Takahashi T, Mitsui Y, Ide T, et al. (2007) Telomerase activation induces elongation of the telomeric single-stranded overhang, but does not prevent chromosome aberrations in human vascular endothelial cells. Biochem Biophys Res Commun. 23; 353(4): 926–32. Epub 2006 Dec 22.
16. Wobser H, Dorn C, Weiss TS, Amann T, Bollheimer C, et al. (2009) Lipid accumulation in hepatocytes induces fibrogenic activation of hepatic stellate cells. Cell Res 19(8): 996–1005. doi:10.1038/cr.2009.73.
17. Lamont RJ, Chan A, Belton CM, Izutsu KT, Vasel D, et al. (1995) Porphyromonas gingivalis invasion of gingival epithelial cells. Infect Immun 63: 3878–3885.
18. Inubushi T, Kawazoe A, Miyauchi M, Kudo Y, Ao M, et al. (2012) Molecular mechanisms of the inhibitory effects of bovine lactoferrin on lipopolysaccharide-mediated osteoclastogenesis. J Biol Chem 287(28): 2 3527–36. doi:10.1074/jbc.M111.324673. Epub 2012 May 16.
19. Fernandez AZ, Siebel AL, El-Osta A (2010) Atherogenic factors and their epigenetic relationships. Int J Vasc Med 2010: 437809 doi:10.1155/2010/437809. Epub 2010 Sep 16.
20. Aas JA, Paster BJ, Stokes LN, Olsen I, Dewhirst FE (2005) Defining the normal bacterial flora of the oral cavity. J Clin Microbiol 43(11): 5721–32.
21. Furusho H, Miyauchi M, Hyogo H, Inubushi T, Ao M, et al. (2013) Dental infection of Porphyromonas gingivalis exacerbates high fat diet-induced steatohepatitis in mice. J Gastroenterol Jan 11. DOI 10.1007/s00535-012-0738-1.
22. Yu Q, Li Y, Waqar AB, Wang Y, Huang B, et al. (2012) Temporal and quantitative analysis of atherosclerotic lesions in diet-induced hypercholesterolemic rabbits. J Biomed Biotechnol 2012: 506159. doi:10.1155/2012/506159. Epub 2012 Mar 14.
23. Boden G (2008) Obesity and free fatty acids. Endocrinol Metab Clin North Am 37(3): 635–46, viii–ix. doi:10.1016/j.ecl.2008.06.007.
24. Piro S, Spampinato D, Spadaro L, Oliveri CE, Purrello, et al. (2008) Direct apoptotic effects of free fatty acids on human endothelial cells. Nutr Metab Cardiovasc Dis 18(2): 96–104. Epub 2007 Jun 8.
25. Graesser D, Solowiej A, Bruckner M, Osterweil E, Juedes A, et al. (2002) Altered vascular permeability and early onset of experimental autoimmune encephalomyelitis in PECAM-1-deficient mice. J Clin Invest 109: 383–392.
26. Muller W, Weigl S, Deng X, Phillips D (1993) PECAM-1 is required for transendothelial migration of leukocytes. J Exp Med 178: 449–460.
27. Carrithers M, Tandon S, Canosa S, Michaud M, Graesser D, et al. (2005) Enhanced susceptibility to endotoxic shock and impaired STAT3 signaling in CD31-deficient mice. Am J Pathol Jan; 166(1): 185–96.
28. Yun PL, Decarlo AA, Chapple CC, Hunter N (2005) Functional implication of the hydrolysis of platelet endothelial cell adhesion molecule 1 (CD31) by gingipains of Porphyromonas gingivalis for the pathology of periodontal disease. Infect Immun. Mar; 73(3): 1386–98.
29. Filippatos G, Ang E, Gidea C, Dincer E, Wang R, et al. (2004) Fas induces apoptosis in human coronary artery endothelial cells in vitro. BMC Cell Biol 22: 5: 6.
30. Maloney E, Sweet IR, Hockenbery DM, Pham M, Rizzo NO, et al. (2009) Activation of NF-kappaB by palmitate in endothelial cells: a key role for NADPH oxidase-derived superoxide in response to TLR4 activation. Arterioscler Thromb Vasc Biol. 2009 Sep; 29(9): 1370–5.
31. Ajuwon KM1, Spurlock ME (2005) Palmitate activates the NF-kappaB transcription factor and induces IL-6 and TNFalpha expression in 3T3-L1 adipocytes. J Nutr. 2005 Aug; 135(8): 1841–6.
32. Collins T, Read M, Neish A, Whitley M, Thanos D, et al. (1995) Transcriptional regulation of endothelial cell adhesion molecules: NF- kappa B and cytokine-inducible enhancers. FASEB J 9: 899–909.
33. Liu SF, Malik AB (2006) NF-kappa B activation as a pathological mechanism of septic shock and inflammation. Am J Physiol Lung Cell Mol Physiol 290(4): L622–L645.
34. Kershaw EE, Flier JS (2004) Adipose tissue as an endocrine organ. J Clin Endocrinol Metab 89(6): 2548–56.
35. Xu H, Barnes GT, Yang Q, Tan G, Yang D, et al. (2003) Chronic inflammation in fat plays a crucial role in the development of obesity-related insulin resistance. J Clin Invest 112(12): 1821–30.
36. Figuero E, Sánchez-Beltrán M, Cuesta-Frechoso S, Tejerina JM, del Castro JA, et al. (2011) Detection of periodontal bacteria in atheromatous plaque by nested polymerase chain reaction. J Periodontol 82(10): 1469–77. doi:10.1902/jop.2011.100719. Epub 2011 Mar 29.

Telomeric G-Tail Length and Hospitalization for Cardiovascular Events in Hemodialysis Patients

Shuma Hirashio, Ayumu Nakashima,* Shigehiro Doi,* Kumiko Anno,† Eriko Aoki,† Akira Shimamoto,† Noriaki Yorioka,‡ Nobuoki Kohno,§ Takao Masaki,* and Hidetoshi Tahara†*

Abstract

Background and objectives Telomeric G-tails play a pivotal role in maintaining the intramolecular loop structure of telomeres. Previous *in vitro* studies have suggested that the erosion of telomeric G-tails triggers cellular senescence, leading to organ dysfunction and atherosclerosis. The authors recently established a method to measure telomeric G-tail length using a hybridization protection assay. Using this method, this study investigated whether telomeric G-tail length could be used as a novel predictor for future cardiovascular events in hemodialysis patients.

Design, setting, participants, & measurements A prospective observational study was performed involving a cohort of 203 Japanese hemodialysis patients to examine the lengths of telomeric G-tails and total telomeres and subsequent cardiovascular events during a median follow-up period of 48 months. The lengths of telomeric G-tails and total telomeres were also measured in 203 participants who did not have CKD and who were age- and sex-matched to hemodialysis patients.

Results The lengths of telomeric G-tails and total telomeres were significantly shorter in hemodialysis patients than in control subjects. Telomeric G-tails, but not total telomeres, were independently and negatively associated with clinical history of cardiovascular disease. During follow-up, 80 cardiovascular events occurred. Total telomere length did not predict cardiovascular events. However, the length of telomeric G-tails was associated with new-onset cardiovascular events (hazard ratio per log luminescence signals, 0.12; 95% confidence interval, 0.12 to 0.50) that persisted after adjustment for age, sex, diabetes mellitus, clinical history of cardiovascular disease, inflammation, use of vitamin D, and serum levels of phosphate and intact parathyroid hormone.

Conclusions Longer telomeric G-tail length is associated with a lower risk of future cardiovascular events in hemodialysis patients.

Clin J Am Soc Nephrol 9: 2117–2122, 2014. doi: 10.2215/CJN.10010913

*Department of Nephrology, Hiroshima University Hospital, Hiroshima, Japan; Departments of †Cellular and Molecular Biology and §Molecular and Internal Medicine, Graduate School of Biomedical & Health Science, Hiroshima University, Hiroshima, Japan; and ‡General Incorporated Association Hiroshima Kidney Organization, Hiroshima, Japan

Correspondence: Dr. Hidetoshi Tahara, Department of Cellular and Molecular Biology, Graduate School of Biomedical Science Hiroshima University, 1-2-3, Kasumi, Minami-ku, Hiroshima, 734-8553, Japan. Email: toshi@hiroshima-u.ac.jp

Introduction

Human telomeres contain 10–15 kilobase pairs of the repeating telomeric DNA sequence, 5′-TTAGGG-3′, followed by 75–300 bases of a G-rich single-stranded 3′ overhang, the so-called G-tail (1).The length of telomeric G-tails plays a pivotal role in maintaining the intramolecular loop structure of the telomere, a structure that is also known as the "t loop" (2). The collapse of the t-loop structure leads to telomere dysfunction and is accompanied by end-to-end fusion of chromosomes. Consequently, this structure is considered to be essential for the maintenance of chromosome terminal structure and function and its assembly into stable protein-telomeric DNA complexes (3). In fact, previous reports have shown that telomeric G-tail erosion, rather than total telomere length, serves as a trigger of cellular senescence and eventually leads to loss of cellular viability *in vitro* (4). We reported that telomeric G-tails in human umbilical vein endothelial cells gradually shortened with cell division and that introduction of the human telomerase reverse transcription (*TERT*) gene rejuvenated cellular functions (5).

Clinical studies have shown that total telomere shortening is associated with increasing chronological age (6,7), progression of arteriosclerosis (8,9), and CKD (10–12). Patients with CKD have a markedly increased risk for cardiovascular disease (CVD) (13) and total telomere shortening is associated with progression of CVD (14). We thus examined whether telomeric G-tail length could be a sensitive marker for CVD in hemodialysis patients. Until recently, no reliable method for the measurement of telomeric G-tail length in clinical samples has been available. However, we recently established a technique to measure telomeric G-tail length using a hybridization protection assay (HPA) (15). In this study, our new method enabled us to measure a large number of clinical samples accurately and with high sensitivity.

Materials and Methods

Participants

We enrolled 203 outpatients receiving maintenance hemodialysis at Hiroshima University Hospital (Hiroshima, Japan), Hakuai Clinic (Kure, Japan), Onomichi Clinic

(Onomichi, Japan), East Clinic (Hiroshima, Japan), and Chuonaika Clinic (Kure, Japan). These patients received dialysis three times a week. Patients with a history of malignant tumor, currently receiving treatment for a malignant tumor, currently receiving steroid therapy, or who were infected at the time of blood sampling were excluded from this study. The clinical history of CVD was also checked by review of medical records at the time of initiating this study. The clinical history of CVD was defined as a previous history of angina pectoris, myocardial infarction, treatment of percutaneous coronary intervention, aortic disease (acute aortic dissection, thoracic aortic aneurysm, or abdominal aortic aneurysm), cerebral hemorrhage, cerebral infarction, or arteriosclerosis obliterans (lower limb amputation, extremity gangrene, or treatment of extremity percutaneous transluminal angioplasty). Afterward, patients were prospectively followed for assessment of a new-onset cardiovascular event in relation to telomeric G-tail length or total telomere length. A new-onset cardiovascular event was defined as angina pectoris, myocardial infarction, treatment of percutaneous coronary intervention, aortic disease (acute aortic dissection, thoracic aortic aneurysm, or abdominal aortic aneurysm), cerebral hemorrhage, cerebral infarction, or arteriosclerosis obliterans (lower limb amputation, extremity gangrene, or treatment of extremity percutaneous transluminal angioplasty during the observational period). These new-onset cardiovascular events were also checked using medical records and, in selected cases, diagnosis by specialists. To assemble control participants for this study, blood samples were obtained from a total of 493 volunteers, 417 of whom were enrolled as participants without CKD based on completion of a medical questionnaire. From that group, 203 samples were assessed for telomeric G-tail and total telomeres as control participants. We selected control participants who were matched with hemodialysis patients for age and sex. The Ethics Committee of our hospitals approved the study protocol (Analysis of Telomere Instability Mechanism in Dialysis Therapy, approval number Hi-129, registered April 2, 2008) and written informed consent was obtained from each patient. This study was conducted in accordance with the Declaration of Helsinki.

Procedures

After PBMCs were isolated from each whole blood sample, DNA was extracted by the modified phenol-chloroform method within 24 hours. Telomeric G-tails and total telomeres were measured by HPA (16). The research staff who measured telomeric G-tails and total telomeres did not know the details regarding clinical data or outcome in this study.

Briefly, the extracted DNA was adjusted to 100 μg/ml using a Nanodrop 2000 spectrophotometer (Thermo Fisher Scientific K.K., Yokohama, Japan), and was subsequently dispensed into three wells of a 96-well plate. The sample plates were set in a JANUS automated workstation (PerkinElmer Japan Co Ltd, Yokohama, Japan) and the HPA reaction was performed. First, a diluted telomere HPA probe labeled with acridinium ester (AE; Fujirebio Inc, Tokyo, Japan) was added to each well, and incubated at 60°C for 20 minutes (hybridization step). Hydrolyzation buffer was then added to each well and samples were incubated at 60°C for 10 minutes (hydrolyzation step). The plate was then set on an EnVision multilabel reader (PerkinElmer Japan Co Ltd) to measure the luminescence of AE. This assay additionally served as a positive control for each HPA using a synthetic 35-mer single-stranded DNA composed of a repeating 5′-(TTAGGG)n-3′ sequence. We measured telomeric G-tail length using 1 μg of purified nondenatured genomic DNA, and total telomere length using 0.2 μg of heat-denatured genomic DNA. Unlike conventional methods such as Southern blotting, telomeric G-tails, and total telomeres are represented as luminescence signals (in relative light units [rlu]) in this technique. We used control genomic DNA isolated from the Henrietta Lacks (HeLa) cancer cell line and control telomere oligonucleotides to normalize the luminescence. To confirm the reliability of HPA, two independent experiments were performed in triplicate. We determined that the average coefficient of variations (CVs) were 4.1% and 4.3% for the telomeric G-tail and total telomeres, respectively.

Laboratory Analyses

Blood samples were collected from hemodialysis patients before the first session of dialysis in a given week. Study parameters were derived from the periodic blood test data collected at the facilities for maintenance dialysis for individual patients. We averaged three consecutive readings during the 2-month period, measuring five parameters: hemoglobin and serum levels of albumin, calcium, phosphate, and C-reactive protein. The adjusted calcium level was calculated by Payne's equation (17). Serum intact parathyroid hormone (PTH) level was measured by electrochemiluminescence immunoassay with the use of the ECLusys reagent PTH (Roche Diagnostics K.K., Tokyo, Japan). Serum β_2 microglobulin levels are shown as the average of two consecutive readings during the 3 months before sampling. Kt/V was calculated with the following single-pool equation: $(Kt/V\ sp = -Ln(Ce/Cs - 0.008 \times td) + (4 - 3.5 \times Ce/Cs) \times \Delta BW/BW)$, where Ce is prehemodialysis urea nitrogen, Cs is posthemodialysis urea nitrogen, ΔBW is weight loss during dialysis, BW is body weight after a session of dialysis, and td is dialysis time (18).

Statistical Analyses

All variables were expressed as the mean±SD or the median and interquartile range (25th–75th percentiles), unless otherwise indicated. Comparisons between two groups were assessed with the Wilcoxon signed-rank test or chi-squared test. Spearman's rank correlation analysis was used to determine possible associations between the lengths of telomeric G-tails or total telomeres with selected parameters. Multivariate regression analyses were used to assess independent predictors of telomeric G-tails and total telomeres, whereas logistic regression approaches were used to assess determinants of existing CVD. Analyses of subsequent cardiovascular events were made with the Cox proportional hazard model. The univariate and multivariate Cox regression analyses are presented as hazard ratios (HRs) and 95% confidence intervals (95% CIs). Statistical significance was set at a level of $P<0.05$. All analyses were carried out with SPSS software (version 21.0; IBM, Armonk, NY).

Results

The clinical characteristics of hemodialysis patients are shown in Table 1. In the patient group, the mean age was 62.7±10.1 years and dialysis duration was 79 (31–138)

months. Diabetes mellitus was present in 86 patients (42.4%), and 88 patients (43.3%) had a history of CVD. Classification of the clinical history of CVD is summarized in Supplemental Table 1. These data were similar to those of general Japanese hemodialysis patients (19). Control subjects included 104 men (51.7%) and the mean age was 62.6±6.2 years. Age and sex did not differ between hemodialysis patients and control participants.

The luminescence signals showed that telomeric G-tails were significantly shorter in length in hemodialysis patients than in control participants (Table 1). Similarly, total telomeres were also significantly shorter in hemodialysis patients than in control participants (Table 1). We previously found that there was a positive correlation between the lengths of telomeric G-tails and total telomeres *in vitro* (5). In this study, we examined the correlation between telomeric G-tail length and total telomere length in control participants and hemodialysis patients. As expected, a strong correlation was observed between telomeric G-tail length and total telomere length in control participants (ρ=0.51, P<0.001) and hemodialysis patients (ρ=0.48, P<0.001).

In univariate analysis (Table 1), there was a positive correlation between telomeric G-tail length and serum phosphate level and a negative correlation between telomeric G-tail length and clinical history of CVD. In addition, total telomere lengths were positively associated with vitamin D use and serum phosphate level, whereas they were negatively associated with age and clinical history of CVD. Next, we performed a multivariate regression analysis of factors associated with the lengths of telomeric G-tails and total telomeres. Table 2 shows the results of multivariate regression analysis of factors predicting telomeric G-tail and total telomere lengths. Specifically, a clinical history of CVD and serum phosphate levels were independently associated with telomeric G-tail length, whereas age and serum phosphate level were independently associated with total telomere length. We also performed an analysis that excluded hemodialysis patients with a history of CVD at baseline (Supplemental Table 2). In this analysis, only serum phosphate levels were independently associated with telomeric G-tail.

Patients with a clinical history of CVD had shorter telomeric G-tail lengths than those without a clinical history of CVD (21,669 rlu [19,162–23,910] for patients with CVD versus 23,078 rlu [20,182–25,972] for patients without CVD; P=0.01). In a logistic regression model, the association remained and was independent of age, sex, diabetes mellitus, serum phosphate level, and inflammation (odds ratios [OR], 0.12 per log rlu; 95% CI, 0.01 to 0.90; P=0.04) (see Telometic G-tail in Table 3). Although patients with a clinical history of CVD had shorter total telomere lengths than those without a clinical history of CVD (218,939 rlu [201,131–242,396] for patients with CVD versus 228,917 rlu [210,971–265,989] for patients without CVD; P=0.01), the association disappeared after adjustments for age, sex, diabetes mellitus, serum phosphate level, and inflammation (see Total telomere in Table 3). See Total telomere, per log rlu in table 3 shows the control of these models (without telomeric G-tail lengths and total telomere lengths).

Cardiovascular events were assessed after a median follow-up period of 48 months (range, 3–57; interquartile

Table 1. General characteristics of hemodialysis patients and healthy controls, and univariate associations with telomeric G-tail and total telomere lengths in patients

Variable	Control Subjects (n=203)	Hemodialysis Patients (n=203)	Telomeric G-Tail ρ	Total Telomere ρ
Telomeric G-tail, rlu	29,511 (26,215–33,040)	22,449 (19,523–25,220)[a]	—	—
Total telomere, rlu	283,756 (252,755–318,617)	226,318 (208,173–258,269)[a]	0.69[b]	—
Age, yr	62.7±6.2	62.7±10.1	−0.32	−0.30
Men	104 (51.7)	106 (52.2)	−0.33	−0.56[b]
Dialysis duration, mo		79 (31–138)	−0.24	−0.22
Diabetes mellitus		86 (42.4)	−0.16	−0.08
History of CVD		88 (43.3)	−0.43[c]	−0.41[d]
Vitamin D use		90 (44.3)	0.29	0.39[d]
Hemoglobin, g/dl		10.3±1.3	−0.22	−0.19
Albumin, g/dl		3.7±0.4	0.18	0.25
Adjusted calcium, mg/dl		9.4±0.8	−0.30	0.06
Phosphate, mg/dl		5.2±1.5	0.43[c]	0.56[b]
Intact PTH, pg/ml		135 (55–229)	0.23	0.46[b]
β2 microglobulin, mg/L		28.5±7.3	−0.19	−0.17
C-reactive protein, mg/dl		0.10 (0.05–0.30)	0.34	−0.29
Kt/V		1.32±0.25	−0.21	0.08

Data are means±SD or median (interquartile range) for continuous variables and n (%) for categorical variables. Univariate correlations were assessed by Spearman's rank correlation analysis. rlu, relative light unit; CVD, cardiovascular disease; PTH, parathyroid hormone.

[a]Significantly different (P<0.05) from healthy individuals as assessed by Wilcoxon signed-rank test or chi-squared test.

[b]P<0.001.

[c]P<0.01.

[d]P<0.05

Table 2. Multivariate regression model predicting telomeric G-tail and total telomere length in 203 hemodialysis patients

Parameter	β	*P* Value	Adjusted r^2
Telomeric G-tail length			0.08
Age, per 1 yr	−0.03	0.67	
Men	−0.10	0.17	
Diabetes mellitus, presence	0.03	0.67	
Clinical history of CVD, presence	−0.16	0.04	
Phosphate, per 1 mg/dl	0.16	0.03	
Inflammation, presence	0.05	0.49	
Total telomere length			0.15
Age, per 1 yr	−0.25	<0.01	
Men	−0.08	0.26	
Diabetes mellitus, presence	0.02	0.74	
Clinical history of CVD, presence	−0.05	0.46	
Phosphate, per 1 mg/dl	0.23	<0.01	
Inflammation, presence	0.02	0.73	

β shows standard regression coefficient. Inflammation was defined as C-reactive protein >0.5 mg/dl.

range, 23–55). During the follow-up period, 80 patients (39.4%) were hospitalized with a new-onset cardiovascular event. Causes of new-onset cardiovascular events are summarized in Supplemental Table 1. Cox proportional hazard crude analyses showed that patients with shorter telomeric G-tail lengths had an increase of new-onset cardiovascular events (HR, 0.12 per log rlu; 95% CI, 0.03 to 0.50; *P*=0.004). This difference persisted after adjustment for age, sex, diabetes mellitus, history of CVD, inflammation, vitamin D use, and serum levels of phosphate and intact PTH (see Telomeric G-tail in Table 4). By contrast, total telomere length was not associated with future cardiovascular events (see Total telomeres in Table 4). After multivariate adjustment, HRs were not statistically significant.

Discussion

In this study, we report for the first time that telomeric G-tail lengths were shortened in hemodialysis patients. The reduction of telomeric G-tail length was associated with future cardiovascular events. The association was independent of age, sex, diabetes mellitus, baseline CVD, vitamin D use, inflammation, and serum levels of phosphate and intact PTH. Our findings indicate that telomeric G-tail length but not total telomere length could be a novel predictor for future cardiovascular events in hemodialysis patients.

Oxidative stress and chronic inflammation are well known risk factors of CVD and play major roles in total telomere shortening (9,20). A previous study demonstrated that patients with CVD had shortening of total telomere length

Table 3. ORs and 95% CI for factors predicting the clinical history of CVD in 203 hemodialysis patients

Parameter	Odds Ratio (95% CI)	*P* Value	Adjusted r^2
Telomeric G-tail			0.16
Age, per 1 yr	1.10 (1.06 to 1.14)	<0.01	
Men	1.14 (0.59 to 2.20)	0.69	
Diabetes mellitus, presence	1.80 (0.93 to 3.52)	0.08	
Phosphate, per 1 mg/dl	1.06 (0.83 to 1.35)	0.65	
Inflammation, presence	0.76 (0.31 to 1.86)	0.56	
Telomeric G-tail, per log rlu	0.12 (0.01 to 0.90)	0.04	
Total telomere			0.15
Age, per 1 yr	1.10 (1.06 to 1.14)	<0.001	
Men	1.18 (0.62 to 2.25)	0.62	
Diabetes mellitus, presence	1.67 (0.87 to 3.20)	0.12	
Phosphate, per 1 mg/dl	1.03 (0.81 to 1.31)	0.81	
Inflammation, presence	0.89 (0.38 to 2.09)	0.80	
Total telomere, per log rlu	0.47 (0.05 to 3.98)	0.48	
Without telomeric G-tail and total telomere			0.14
Age, per 1 yr	1.10 (1.06 to 1.14)	<0.01	
Men	1.18 (0.62 to 2.23)	0.61	
Diabetes mellitus, presence	1.71 (0.90 to 3.26)	0.10	
Phosphate, per 1 mg/dl	0.98 (0.78 to 1.24)	0.89	
Inflammation, presence	0.84 (0.36 to 1.94)	0.68	

Inflammation was defined as C-reactive protein >0.5 mg/dl. OR, odds ratio; 95% CI, 95% confidence interval.

Table 4. Hazard ratios for telomeric G-tail length and total telomere length with cardiovascular events in patients

Model	Covariate	Cardiovascular Events	
		HR (95% CI)	*P* Value
Telomeric G-tail			
1	Crude (per log rlu)	0.12 (0.03 to 0.50)	0.004
2	1 plus age, sex, and diabetes mellitus	0.16 (0.04 to 0.65)	0.01
3	2 plus baseline CVD and inflammation	0.18 (0.04 to 0.78)	0.02
4	3 plus vitamin D use, phosphate, and intact PTH	0.14 (0.03 to 0.63)	0.01
Total telomeres			
1	Crude (per log rlu)	0.39 (0.08 to 1.31)	0.12
2	1 plus age, sex, and diabetes mellitus	0.50 (0.11 to 2.14)	0.35
3	2 plus baseline CVD and inflammation	0.48 (0.11 to 2.11)	0.33
4	3 plus vitamin D use, phosphate, and intact PTH	0.25 (0.05 to 1.28)	0.10

Indicated are crude HRs or with various degrees of adjustment (models 2–4) for cardiovascular events according to telomeric G-tail and total telomere length. Inflammation was defined as C-reactive protein >0.5 mg/dl. HR, hazard ratio.

compared with healthy participants (21). Notably, previous reports have found that total telomere shortening *per se* causes cellular senescence in vascular endothelial cells (22) and eventually leads to atherosclerotic plaques (23). It raises the possibility that shortening of total telomere length directly involves pathologic conditions of CVD through cellular senescence.

However, there have been no studies that showed a correlation between total telomere length and the incidence of CVD in hemodialysis subjects. This study revealed that telomeric G-tail length (but not total telomere length) independently predicted new-onset cardiovascular events in hemodialysis patients. Telomere length is well correlated with G-tail length under normal conditions; however, we found a link between G-tail and CVD event, but not total telomere length. This result is similar to our previous report of *in vitro* experiments using a G-quadruplex inhibitor that induced telomere dysfunction by t-loop destruction (24). Therefore, we postulate that G-tail reduction in patients with CKD is due to oxidative stress exposure. A possible explanation is that oxidative stress has a predilection for a guanine-rich single-stranded 3′ overhangs of G-tails (25). Although sherterin components play an important role in t-loop formation and protection (26), past studies did not establish a link between those proteins and CKD. These results suggest that telomeric G-tail length may be a sensitive marker for CVD in patients with CKD.

Our data show that both telomeric G-tail length and total telomere length in hemodialysis patients were shorter than those in control participants. Telomeric G-tail and total telomere shortening in aging healthy individuals is mainly caused by cell division, whereas other factors such as oxidative stress and inflammation might contribute to telomeric G-tail shortening in hemodialysis patients. In fact, it was reported that total telomere length is shorter in CKD before starting RRT (27). It is therefore likely that kidney insufficiency, rather than hemodialysis therapy, contributes to shortened telomeric DNA.

In addition to the clinical history of CVD, increased phosphate levels showed a significant correlation with both telomeric G-tail length and total telomere length, suggesting that high phosphate reduced telomere shortening. However, previous studies suggested that dysfunctional phosphate metabolism in hemodialysis patients increased CVD events and mortality (28). This discrepancy might be because patients with high phosphate levels are also highly active (29). In fact, shortened telomeres are reportedly associated with low levels of physical activity (30).

We previously developed the HPA to measure telomeric G-tail length in many clinical samples of PBMCs (15). Telomeric G-tail length and total telomere length measurement by HPA does not include subtelomeric sequences because the AE-labeled probes are quite specific. Actual telomeric G-tail length and total telomere length can be compared with conventional methods using a radioisotope assay (15,31). By contrast, conventional methods are semiquantitative because telomeric G-tail length is measured by densitometry of the smear pattern of an autoradiogram. In this article, we used a modified G-tail telomere HPA, and CV values were better than the original assay. Therefore, the method used in this study is a reliable technique for measurement of telomeric G-tail and telomere lengths.

The strengths of our observational study include its prospective design, the large number of clinical samples from hemodialysis patients, the long duration of follow-up, measurement by an accurate method, and the ability to adjust for various important risk factors. By contrast, some limitations of our study merit comment. Although PBMCs provide an easily accessible source for DNA analysis, it is not clear whether telomeric G-tail length in PBMCs reflects that in tissues. Although the methods used for the assessments of telomeric G-tail and total telomere lengths in this study are reliable, the average CVs of those measurements were relatively wide. Because our cohort comprises Japanese hemodialysis patients, our results may not necessarily be generalizable to other populations.

This is the first study to report simultaneous measurements of telomeric G-tail length and total telomere length in hemodialysis patients. This study shows that telomeric G-tail length is shortened in hemodialysis patients. Telomeric G-tail length of hemodialysis patients is also associated with CVD history and the likelihood of future hospitalization for a cardiovascular event.